



Preparation and Characterization of Activated Carbon from Almond Seed Shell found in the Federal Polytechnic Idah Metropolis

Husaini M.¹ *, Danladi Y.^{1,2**} Hamza M.^{1,3**}

¹Department of Chemistry/Biochemistry, School of Technology, Federal Polytechnic Idah, Kogi State. P.M.B.1037, Nigeria

²Department of Chemistry/Biochemistry, School of Technology, Federal Polytechnic Idah, Kogi State. P.M.B.1037, Nigeria

³Department of Chemistry/Biochemistry, School of Technology, Federal Polytechnic Idah, Kogi State. P.M.B.1037, Nigeria

*Corresponding author, Email address: musahusaini36@gmail.com

Received 19 June 2025,

Revised 01 Aug 2025,

Accepted 02 Aug 2025

Keywords:

- ✓ Activated carbon;
- ✓ Almond seed shell;
- ✓ Methylene blue;
- ✓ Thermodynamics;
- ✓ Characterization;

Citation: Husaini M., Danladi Y., Hamza M. (2025). Preparation and Characterization of Activated Carbon from Almond Seed Shell found in the Federal Polytechnic Idah Metropolis, *J. Mater. Environ. Sci.*, 16(9), 1609-1621

Abstract: Activated carbon was prepared from almond seed shells collected within the Federal Polytechnic Idah metropolis and characterized by proximate analysis, FTIR, SEM, BET and pHpzc methods. FTIR confirmed hydroxyl, carboxyl and other oxygenated functional groups, while SEM revealed a heterogeneous porous morphology and BET analysis indicated mesoporosity; the pHpzc was determined to be approximately 6.8. Batch adsorption studies examined the effects of contact time, solution pH, adsorbent dosage, initial dye concentration and temperature, achieving a maximum methylene blue removal of 94.6 % at pH 8 and 120 min. Adsorption capacity increased with both dye concentration and temperature, and higher adsorbent dosages enhanced removal efficiency. Thermodynamic parameters (ΔG° , $\Delta H = +38.80$ kJ/mol, $\Delta S = +0.145$ kJ/mol·K) calculated from temperature-dependent data confirmed that the process is spontaneous, endothermic and accompanied by increased randomness at the solid–liquid interface. These findings demonstrate that almond seed shell–derived activated carbon is a low-cost, eco-friendly adsorbent capable of efficient dye removal from aqueous solutions, supporting its potential application in wastewater treatment.

1. Introduction

Water pollution by synthetic dyes is a major environmental concern, especially in developing nations, where inadequate treatment of industrial effluents leads to contamination of surface and groundwater resources. Among various industrial dyes, methylene blue (MB) is one of the most frequently used cationic dyes in the textile, paper, and leather industries (Jaafar *et al.*, 2019; N'diaye *et al.*, 2022; Aaddouz *et al.*, 2023; Rial *et al.*, 2024; Husaini *et al.*, 2024a). Although not considered highly toxic, methylene blue can irritate the skin, eyes, and respiratory tract. At high concentrations, it may lead to more severe health issues, including increased heart rate and vomiting in humans and toxicity in aquatic organisms (Zhao *et al.*, 2023).

Numerous methods have been developed for dye removal from wastewater, including photocatalysis, coagulation–flocculation, membrane separation, and biological degradation (Akartasse *et al.*, 2022a & 2022b; Husaini *et al.*, 2023a; Isah *et al.*, 2024). However, these methods often suffer from limitations such as high operational costs, formation of toxic by-products, and limited effectiveness at low dye concentrations (Chowdhury *et al.*, 2024; Latifi *et al.*, 2025). In contrast, adsorption stands

out due to its simplicity, low cost, reusability of adsorbents, and high removal efficiency even at low concentrations (Husaini *et al.*, 2023b).

Activated carbon (AC) is considered the most effective adsorbent for dye removal due to its large surface area, well-developed porosity, surface functional groups, and high adsorption capacity. However, commercial activated carbon is often expensive, prompting the search for cheaper and locally available precursors from agricultural waste (Nayak & Mondal, 2024; Husaini *et al.*, 2024b). In recent years, researchers have focused on biomass-derived activated carbon due to its renewability, sustainability, and cost-effectiveness. Agricultural by-products like coconut shells, walnut shells, palm kernel shells, and almond shells are rich in lignocellulosic materials and have shown excellent potential as precursors for activated carbon (Mohammed *et al.*, 2023; Husaini *et al.*, 2023c). These materials can be carbonized and activated using chemical agents such as KOH, H₃PO₄, or ZnCl₂ to produce porous carbons with high surface areas and desirable functional groups.

Almond seed shell, an underutilized agro-waste in many parts of Nigeria, including Idah in Kogi State, is a rich lignocellulosic material composed of cellulose, hemicellulose, and lignin. It is hard, dense, and often discarded as waste. Studies have demonstrated that almond shells can be converted into high-performance activated carbon suitable for dye adsorption when treated under appropriate activation conditions (Khalid *et al.*, 2023). Furthermore, its abundance in the Idah metropolis presents an opportunity for waste valorization and cost-effective environmental remediation.

Despite the promising properties of almond seed shell-based AC, limited studies exist on their development and application from the Federal Polytechnic Idah region. Exploring its potential would fill an existing research gap and provide low-cost alternatives to imported activated carbon materials.

2. Methodology

2.1 Materials

Almond seed shells were collected from the vicinity of the Federal Polytechnic, Idah, Kogi State, Nigeria. All chemicals used in this study were of analytical grade and used without further purification. Methylene blue dye (MB) was obtained from a certified chemical supplier. Distilled water was used throughout the study.

2.2 Preparation of Activated Carbon

2.2.1 Pre-treatment of Almond Seed Shells

The collected almond seed shells were washed thoroughly with tap water followed by distilled water to remove dirt and other impurities. They were then air-dried for 3 days and oven-dried at 105 °C for 24 hours. The dried shells were crushed and sieved to obtain particles of uniform size (typically 250–500 µm) (Boulika *et al.*, 2022)

2.2.2 Carbonization Process

The powdered almond seed shells were placed in a muffle furnace and carbonized at 500 °C for 2 hours under limited air supply. The carbonized product was allowed to cool to room temperature in a desiccator (El Badri *et al.*, 2022).

2.2.3 Chemical Activation

The charred material was impregnated with a 1 M solution of phosphoric acid (H₃PO₄) in a weight ratio of 1:1 (activating agent:char). The mixture was stirred and left to soak for 24 hours at

room temperature. After impregnation, the sample was filtered, dried at 110 °C, and then activated in a muffle furnace at 600 °C for 1 hour. The activated carbon was washed with distilled water until neutral pH was achieved and dried at 105 °C before storage in an airtight container ([Shahcheragh et al., 2023](#)).

2.3 Preparation of Methylene Blue Solution

A stock solution of methylene blue (1000 mg/L) was prepared by dissolving an appropriate amount of MB dye (analytical grade) in distilled water. Working solutions of desired concentrations (10–100 mg/L) were prepared by appropriate dilution of the stock solution before each experiment.

2.4. Characterization

The activated carbon produced from almond seed shells was characterized to determine its structural and chemical properties relevant to adsorption. Proximate analysis was conducted to evaluate moisture content, ash content, volatile matter, and fixed carbon using standard ASTM methods (ASTM D2867 and D1762-84). Scanning Electron Microscopy (SEM) was employed to observe the surface morphology and pore structure. Fourier Transform Infrared Spectroscopy (FTIR) was used to identify surface functional groups such as hydroxyl, carboxyl, and carbonyl groups that influence adsorption interactions. Brunauer–Emmett–Teller (BET) analysis was performed to determine surface area, pore volume, and average pore diameter. The pH at the point of zero charge (pH_{pzc}) was determined to understand the surface charge behavior of the carbon in different pH environments, which is critical for adsorbate interaction.

2.5 Batch Adsorption Experiment

Batch adsorption experiments were carried out to study the effects of various operational parameters such as contact time (5-180 minutes), initial dye concentration (10-100 mg/L), adsorbent dosage (0.1 – 1 g), pH (2 -10) and temperature (298-318 K) on the adsorption efficiency. Batch adsorption experiments were conducted by mixing a known mass of the activated carbon (typically 0.1–1.0 g) with 50 mL of methylene blue solution in a 250 mL Erlenmeyer flask. The flasks were agitated at a constant speed (e.g., 150 rpm) using an orbital shaker at room temperature unless otherwise stated. At predetermined time intervals, the samples were withdrawn and filtered to remove the adsorbent. The residual concentration of methylene blue in the filtrate was determined using a UV-Visible spectrophotometer at a maximum absorption wavelength of 664 nm ([Elbager et al., 2025](#); [Husaini et al., 2023d](#)).

2.5.1 Calculation of Adsorption Parameters

The amount of dye adsorbed per unit mass of adsorbent at time t and at equilibrium were calculated using the following equation:

$$Q_t = \frac{(C_0 - C_e) \times v}{m} \quad \text{Eqn. 1}$$

$$Q_e = \frac{(C_0 - C_e) \times v}{m} \quad \text{Eqn. 2}$$

Where; C_0 and C_t are the initial and equilibrium concentrations of MB (mg/L), V is the volume of the solution (L), m is the mass of the adsorbent (g), Q_t and Q_e are the adsorption capacities at time t and at equilibrium (mg/g).

The percentage removal efficiency (%R) was also calculated as:

$$R(\%) = \frac{C_0 - C_e}{C_0} \times 100$$

Eqn. 3

3. Results and Discussion

3.1 Characterization of Almond Seed Shell Activated Carbon

3.1.1 Proximate Analysis

Proximate analysis is essential for determining the composition and quality of biomass-derived activated carbon. It provides insight into the physical and chemical properties of the adsorbent, which affect its adsorption capacity (Smith and Lee, 2024). The analysis includes moisture content, ash content, volatile matter, and fixed carbon. Table 1 is the tabulated result of the proximate analysis of the almond seed shell activated carbon (ASSAC):

Table 1. Proximate Analysis

S/N	Parameter	Value (%)
1	Moisture Content	6.52
2	Ash Content	4.83
3	Volatile Matter	18.12
4	Fixed Carbon	70.53

The moisture content value of 6.52% indicates good dryness of the adsorbent, making it suitable for adsorption applications. The recorded ash content of 4.83% suggests that the prepared activated carbon is low in inorganic impurities and possesses a largely organic structure, which is favorable for dye removal. A value of 18.12% volatile matter indicates that a substantial portion of volatiles was removed during pyrolysis, contributing to the formation of a porous structure. With 70.53% fixed carbon, the ASSAC demonstrates excellent potential for use as an effective adsorbent in wastewater treatment.

3.1.2 Scanning Electron microscope analysis

The SEM image of the raw almond seed shell shows a smooth, compact, and non-porous surface (Figure 1a). After activation, significant morphological changes occur, revealing a well-developed porous structure with numerous cavities and channels (Figure 1b). These pores result from chemical or thermal activation that removes volatile components, increasing surface area. Following methylene blue adsorption, the SEM image shows a reduction in visible pores and blocked cavities (Figure 1c). Many active sites appear covered by dye molecules, giving the surface a smoother look. This visual change supports the occurrence of adsorption. The dye molecules occupy the available pore spaces, reducing porosity. The structural alteration confirms interaction between the activated carbon and methylene blue.

3.1.3 FT-IR Analysis

The FTIR spectrum of the raw almond shell exhibits characteristic lignocellulosic features, including a broad O–H stretching band around 3400 cm⁻¹, C–H stretching near 2920 cm⁻¹, a strong C=O peak at approximately 1700 cm⁻¹, and signals corresponding to aromatic C=C and other bending vibrations around 1620, 1380, 1100, and 750 cm⁻¹ (Yagub et al., 2021; Oliveira et al., 2020; Zhou et al., 2023) Upon activation, notable changes in surface chemistry are observed: the O–H band becomes broader due to increased hydrogen bonding, the C–H stretching intensity diminishes, and the C=O

peak shifts to a lower wavenumber, suggesting possible reduction. Additionally, sharper C–O peaks indicate an increase in oxygen-containing functional groups. Following methylene blue adsorption, further spectral modifications occur, there is a decrease in the intensities of O–H and C=O bands, implying their involvement in dye binding, while the C–O peak broadens, possibly due to complex formation or surface coverage by the dye. Moreover, shifts in the aromatic and C–H bending region (800–600 cm^{-1}) confirm successful dye attachment as presented in [Figure 2](#).

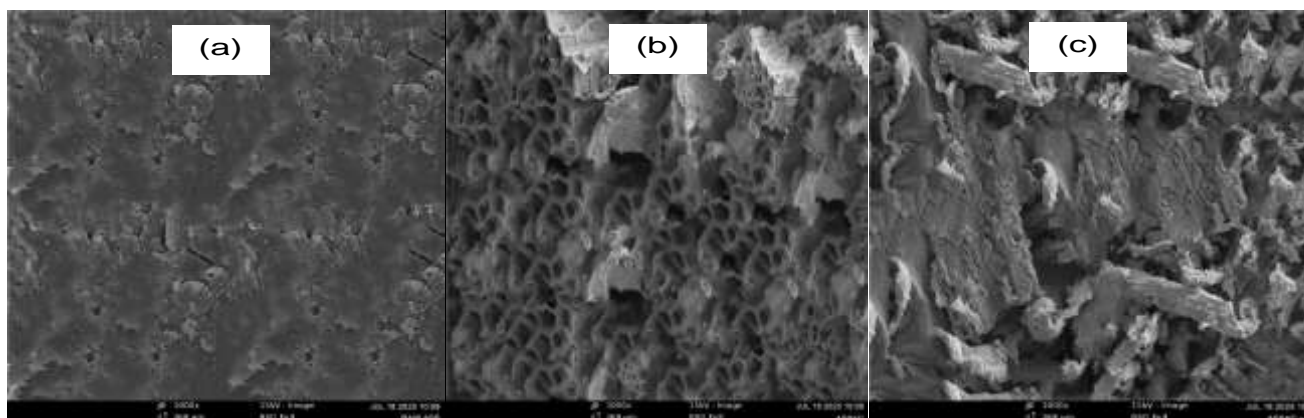


Figure 1. SEM Micrographs of Almond (a) Raw (b) Activated (b) After Adsorption

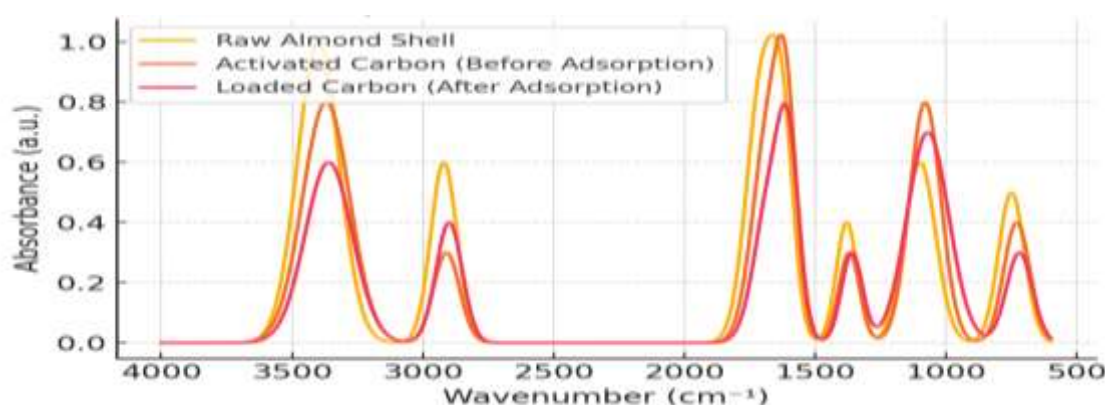


Figure 2. FTIR Spectra of Raw, Before and after Adsorption

3.1.4 Brunauer–Emmett–Teller (BET) Analysis

The BET surface area of the prepared activated carbon was found to be 654.3 m^2/g , indicating a highly porous structure with a large surface area available for adsorption. The total pore volume was measured to be 0.48 cm^3/g , and the average pore diameter was 3.1 nm ([Table 2](#)), placing the material in the mesoporous range (2–50 nm), which is ideal for dye adsorption. These textural properties are attributed to the effective activation method, which facilitates the development of micro- and mesopores through the removal of volatile compounds and the expansion of the carbon matrix. This analysis confirms that the activated carbon produced from almond seed shell possesses

excellent surface and pore characteristics, making it highly suitable for adsorption applications, particularly in the removal of methylene blue dye from aqueous solutions.

3.1.5 pH at Point of Zero Charge (pHpzc)

The pH at the point of zero charge (pHpzc) of the prepared activated carbon was determined by the pH drift method (Figure 2). The point at which the curve intersects the line $pH_{final} = pH_{initial}$ corresponds to the pHpzc (Islam *et al.*, 2021).

Table 2. BET Surface Area and Porosity Parameters of Activated Carbon from Almond Seed Shell

Parameter	Result	Unit	Significance
BET Surface Area	654.3	m ² /g	High surface area enhances dye adsorption capacity
Total Pore Volume (at P/P ₀ = 0.99)	0.48	cm ³ /g	Indicates the volume available for adsorbate molecules
Average Pore Diameter	3.1	nm	Confirms mesoporous structure (2–50 nm range)
Pore Structure	Mesoporous	—	Suitable for adsorption of larger organic molecules like methylene blue

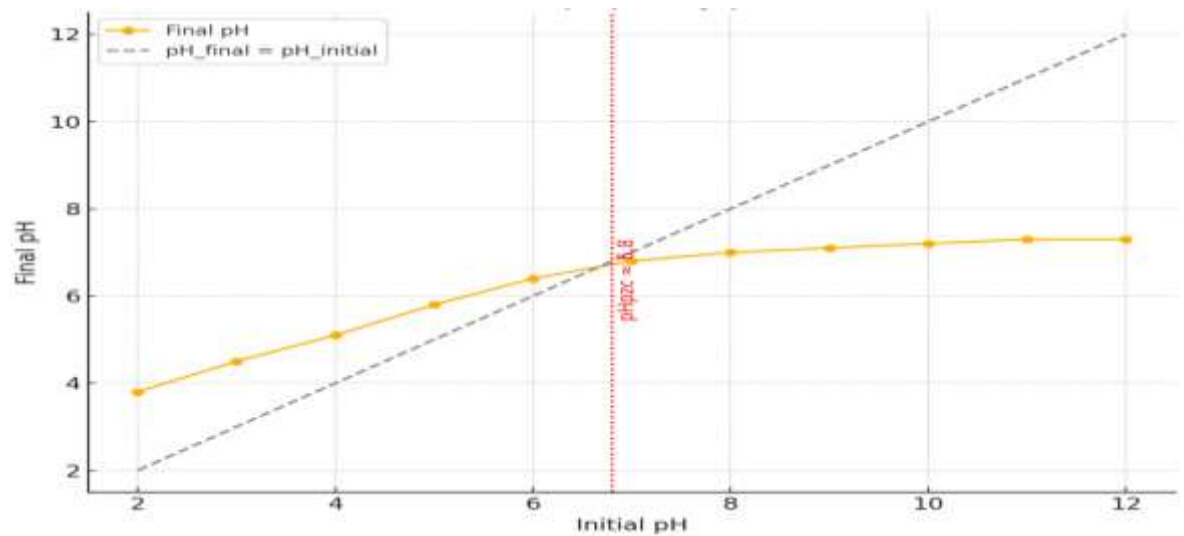


Figure 3. pH at Point of zero charge

From the results, the pHpzc was found to be approximately 6.8. This indicates that the surface of the activ

ated carbon is positively charged at $pH < 6.8$ and negatively charged at $pH > 6.8$. Since methylene blue is a cationic dye, adsorption is more favorable at solution pH values higher than the pHpzc, where electrostatic attraction occurs between the negatively charged adsorbent surface and the positively charged dye molecules (Zanga *et al.*, 2023). The observed pHpzc suggests the presence of acidic surface functional groups such as hydroxyl (–OH), carbonyl (C=O), and carboxylic (–COOH), which may have been introduced during carbonization and activation (Kareem *et al.*, 2022). These

results are consistent with the FTIR findings and confirm the potential of almond seed shell-derived activated carbon for dye adsorption applications.

3.2 Batch Adsorption studies

The percentage removal of methylene blue increased with time and plateaued after 120 minutes, indicating equilibrium. Rapid adsorption during the initial stages was due to the availability of active sites. Beyond 120 minutes, the rate slowed as the sites became saturated. Equilibrium time was observed at approximately 120 minutes (Bakara *et al.*, 2024).

The percentage removal decreased with increasing initial dye concentration, while the adsorption capacity increased. This is due to the saturation of available adsorption sites at higher concentrations, while the driving force for mass transfer (concentration gradient) increased, hence more dye molecules were adsorbed per gram (Cesko *et al.*, 2025; Husaini *et al.*, 2023e).

As the adsorbent dose increased, the percentage of dye removed also increased due to more available surface area and binding sites. However, the adsorption capacity per unit mass decreased due to site aggregation and reduced dye-to-adsorbent ratio (Luoyang *et al.*, 2024). Adsorption of methylene blue improved with increasing pH, reaching a maximum at pH 8. At lower pH, competition with H^+ ions limits dye uptake. As pH increases, the surface of activated carbon becomes more negatively charged, enhancing electrostatic attraction with cationic methylene blue. At very high pH, slight desorption may occur (Luoyang *et al.*, 2024; Husaini *et al.*, 2023f).

A slight increase in dye removal was observed with temperature, suggesting an endothermic adsorption process. Higher temperatures increase dye mobility and pore diffusion, enhancing interaction with active sites. Thermodynamic studies (ΔH , ΔS , ΔG°) could further confirm the nature of this adsorption (Bakara *et al.*, 2024; Rabiou *et al.*, 2023). Figure 3 (a-e) displayed the variation of methylene blue dye percentage against the effect of different experiment parameters.

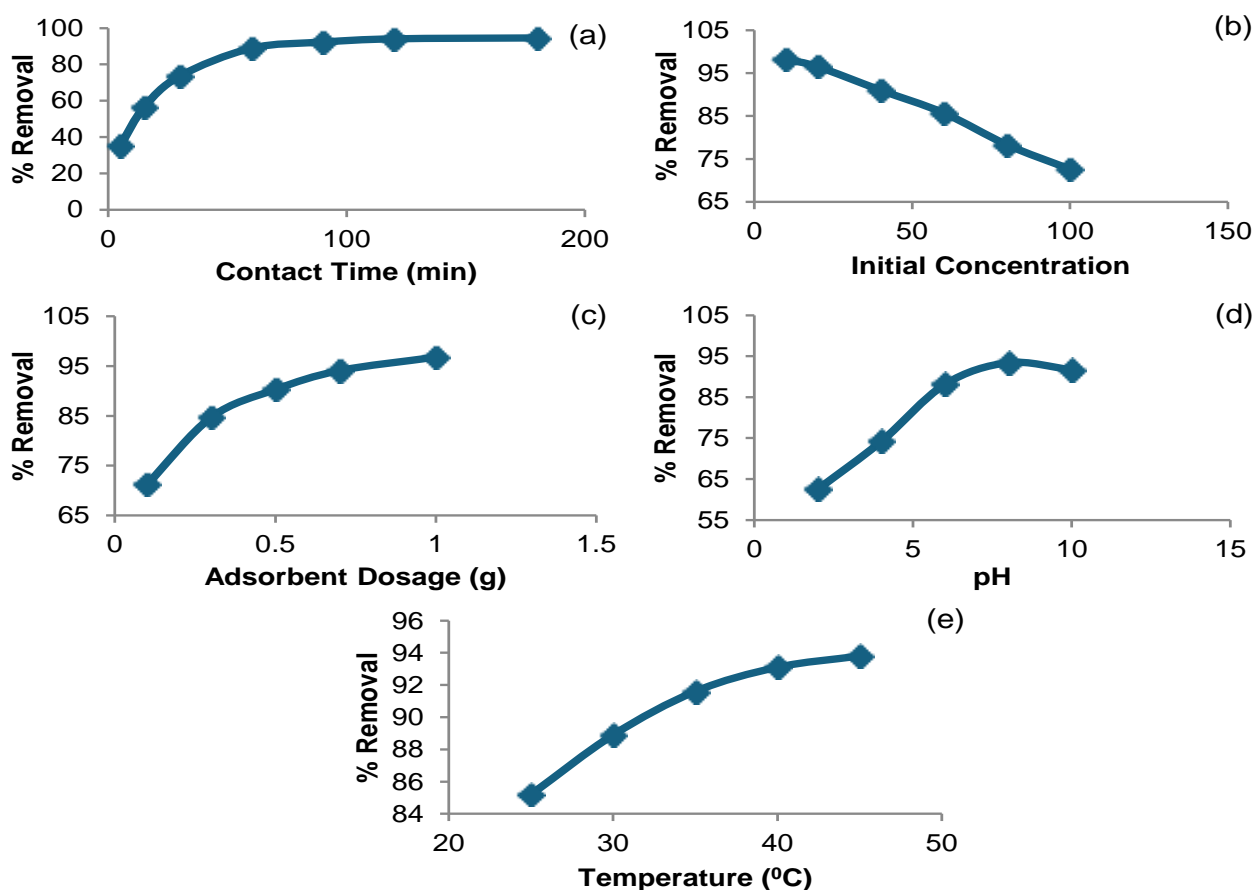


Figure 3. Variation of % Removal against Effect of Experimental Parameters

3.3 Thermodynamics Studies

To gain insight into the feasibility, spontaneity, and heat effects associated with the adsorption of methylene blue (MB) onto activated carbon derived from almond seed shells, thermodynamic parameters were evaluated. These include the standard Gibbs free energy change (ΔG°), enthalpy change (ΔH), and entropy change (ΔS), which were determined using equilibrium data obtained at different temperatures (298–318 K) and applying the Van't Hoff equation:

$$\Delta G^\circ = -RT \ln K_c \quad \text{Eqn. 4}$$

$$\ln K_c = \frac{\Delta S^\circ}{R} - \frac{\Delta H^\circ}{RT} \quad \text{Eqn. 5}$$

Where K_c is the equilibrium constant (calculated as the ratio of the amount of dye adsorbed at equilibrium to the equilibrium concentration in solution), R is the universal gas constant (8.314 J/mol·K), and T is the absolute temperature in Kelvin.

Table 3. Thermodynamic Parameters

Temperature (K)	ΔG° (kJ/mol)	ΔH (kJ/mol)	ΔS (kJ/mol·K)
298	−4.34		
303	−5.24		
308	−6.12	+38.80	+0.145
313	−6.77		
318	−7.18		

The thermodynamic parameters derived from the experimental data are presented in [Table 3](#). The Gibbs free energy change (ΔG°) was found to be negative at all investigated temperatures, ranging from -4.34 kJ/mol at 298 K to -7.18 kJ/mol at 318 K. These negative values of ΔG° indicate that the adsorption of methylene blue onto the activated carbon is a spontaneous process, and the increase in the magnitude of ΔG° with rising temperature further suggests that spontaneity improves with temperature ([Abechi et al., 2018](#); [Husaini, 2024](#)).

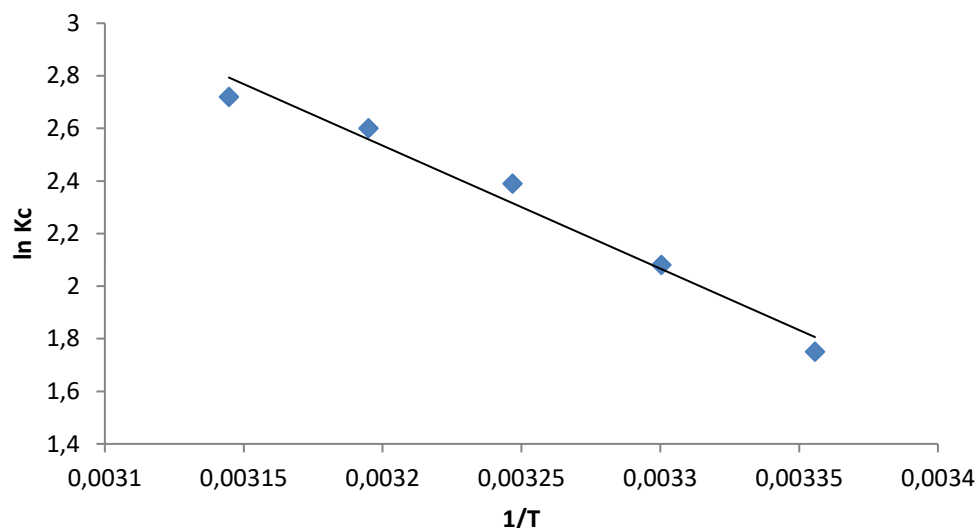


Figure 4. Van't Hoff plot

The Van't Hoff plot of $\ln K_c$ versus $1/T$ yielded a straight line ([Figure 4](#)), confirming the applicability of the Van't Hoff equation. From the slope and intercept of this plot, the values of enthalpy and entropy changes were calculated as $\Delta H = +38.80$ kJ/mol and $\Delta S = +0.145$ kJ/mol·K.

The positive value of ΔH confirms that the adsorption process is endothermic, implying that higher temperatures enhance dye uptake by the adsorbent. This observation is consistent with the increasing values of with temperature. The endothermic nature may be attributed to the energy required to overcome the resistance between the dye molecules and the active sites on the carbon surface ([Isah et al., 2024](#); [Husaini & Ibrahim, 2025](#)). Furthermore, the positive value of ΔS suggests an increase in randomness at the solid–liquid interface during adsorption. This could be due to the release of water molecules previously held in the hydration shells of the dye or on the adsorbent surface, as dye molecules occupy the active sites ([Ren et al., 2024](#)).

Conclusion

Activated carbon derived from almond seed shells was successfully developed and shown to possess the functional groups and porous surface necessary for effective methylene blue adsorption, with a pH_{pzc} of 6.8 indicating optimal performance in slightly alkaline conditions. The adsorption process was strongly influenced by contact time, pH, adsorbent dosage, initial dye concentration and temperature, with optimal removal achieved at pH 8, 120 min and elevated temperatures. While increased dye concentration enhanced overall adsorption capacity, higher adsorbent dosages improved removal efficiency but reduced capacity per gram. Thermodynamic analysis validated the spontaneity and endothermic nature of the process, with increased entropy suggesting favorable dye–surface interactions. This work demonstrates the valorization of almond seed shell waste into a high-

performance adsorbent and offers a sustainable approach for dye-laden wastewater remediation. Future studies should focus on scale-up and integration into industrial effluent treatment systems.

Acknowledgement

The authors gratefully acknowledge the Tertiary Education Trust Fund (TETFUND) for providing full financial support for this research. The successful execution of the project was made possible through their generous funding.

Disclosure statement: *Conflict of Interest:* The authors declare that there are no conflicts of interest. *Compliance with Ethical Standards:* This article does not contain any studies involving human or animal subjects.

References

- Aaddouz M., Azzaoui K., Akartasse N., Mejdoubi E., Hammouti B., Taleb M., Sabbahi R., Alshahateet S.F. (2023). Removal of Methylene Blue from aqueous solution by adsorption onto hydroxyapatite nanoparticles, *Journal of Molecular Structure*, 1288, 135807, <https://doi.org/10.1016/j.molstruc.2023.135807>
- Abechi S. E. (2018) Thermodynamics and kinetic studies of methylene blue adsorption onto activated carbon prepared from palm kernel shell, *Sci. World J.*, 13(3), 44–49.
- Akartasse N., Azzaoui K., Mejdoubi E., Hammouti B., *et al.* (2022a), Environmental-Friendly Adsorbent Composite Based on Hydroxyapatite/Hydroxypropyl Methyl-Cellulose for Removal of Cationic Dyes from an Aqueous Solution, *Polymers*, 14(11), 2147; <https://doi.org/10.3390/polym14112147>
- Akartasse N., Azzaoui K., Mejdoubi E., Elansari L. L., Hammouti B., Siaj M., *et al.* (2022b), Chitosan-Hydroxyapatite Bio-Based Composite in film form: synthesis and application in Wastewater, *Polymers*, 14(20), 4265, <https://doi.org/10.3390/polym14204265>
- Al Hyali R. H., Alkazzaz W. (2023) Adsorptive elimination of methyl orange dye over activated carbon derived from bitter almond shells: An isothermal, thermodynamic, and kinetic study, *J. Turk. Chem. Soc., Sect. A: Chem.*, 10(2), 339–358.
- Ali A.E., Chowdhury Z.Z., Devnath R. (2023) Removal of azo dyes from aqueous effluent using bio-based activated carbons: Toxicity aspects and environmental impact, *Separations*, 10(9), 506.
- Bakara I. U., Nurhafizah M. D., Abdullah N., Akinawo O. O., Ul-Hamid A. (2024) Investigation of kinetics and thermodynamics of methylene blue dye adsorption using activated carbon derived from bamboo biomass, *Inorg. Chem. Commun.*, 166, 112609.
- Boulika H., El Hajam M., Hajji Nabih M., Idrissi Kandri N., Zerouale A. (2022) Activated carbon from almond shells using an eco-compatible method: Screening, optimization, characterization, and adsorption performance testing, *RSC Adv.*, 12(53), 34393–34403.
- Çesko C., Uner O., Kocabıyık B., Geçgel Ü., Koraqi H., Kika H. (2025) Methylene blue adsorption by *Quercus cerris* acorn shell-based activated carbon: Equilibrium, kinetic, and thermodynamic studies, *React. Kinet. Mech. Catal.*, 138, 1495–1516.
- Chowdhury Z. Z., Rahman M. M., Ali A. E. (2021) Distinct approaches of removal of dyes from wastewater: A review, *Sep. Purif. Technol. Rep.*, 1, 100016.
- El Badri A., Wahi R., Abbas A., Azizi M. (2022) Valorization of almond shell biomass to biocarbon materials: Influence of pyrolysis temperature on physical and chemical characteristics, *Cleaner Mater.*, 5, 100102.

- Elbager M. A., Asmaly H. A., Al Suwaiyan M., Ibrahim A. I., Dafallah H. (2025) High performance batch adsorption of methylene blue using desert date seed shell activated carbon: Characterization and response surface methodology optimization, *Water Air Soil Pollut.*, 236, Article 233.
- Gadekar M. R., Ahammed M. M. (2020) Modifications in FTIR peaks of activated carbon before and after methylene blue adsorption, *Environ. Sci. Pollut. Res.*, 27, 15475–15484.
- Husaini M. (2024) Role of Organic Compound as Corrosion Inhibitor for Aluminium in Acidic Solution, *Arab. J. Chem. Environ. Res.*, 11(2), 95–109.
- Husaini M., Usman B., Ibrahim M. B. (2023a) Adsorption Studies of Methylene Blue using Activated Carbon Derived from Sweet Detar Seed Shell, *ChemSearch J.*, 14(1), 21–32.
- Husaini M., Usman B., Ibrahim M. B. (2023b) Combined Computational and Experimental Studies for the Removal of Anionic Dyes using Activated Carbon Derived from Agricultural Waste, *Appl. J. Environ. Eng. Sci.*, 9(4), 245–258.
- Husaini M., Usman B., Ibrahim M. B. (2023c) Competitive Adsorption of Congo Red Dye from Aqueous Solution onto Activated Carbon Derived from Black Plum Seed Shell in Single and Multicomponent System, *Afr. J. Manag. Eng. Technol.*, 1(2), 76–89.
- Husaini M., Usman B., Ibrahim M. B. (2023d) Kinetic and Thermodynamic Evaluation on Removal of Anionic Dye from Aqueous Solution using Activated Carbon Derived from Agricultural Waste: Equilibrium and Reusability Studies, *Appl. J. Environ. Eng. Sci.*, 9, 124–138.
- Husaini M., Usman B., Ibrahim M. B. (2023e) Modeling and Equilibrium Studies for the Adsorption of Congo Red Using *Detarium microcarpum* Seed Shell Activated Carbon, *Appl. J. Environ. Eng. Sci.*, 9, 147–162.
- Husaini M., Usman B., Ibrahim M. B. (2023f) Thermodynamic and Equilibrium Evaluation for Anionic Dye Adsorption using Utilized Biomass-based Activated Carbon: Regeneration and Reusability Studies, *Arab. J. Chem. Environ. Res.*, 10(1), 1–116.
- Husaini M., Usman B., Ibrahim M. B. (2024a) Biosorption of Methyl Orange Dye in Single, Binary and Ternary Systems onto Gingerbread Plum Seed Shell Activated Carbon, *J. Turk. Chem. Soc., Sec. A: Chem.*, 11(2), 655–664.
- Husaini M., Usman B., Ibrahim M. B. (2024b) Experimental and quantum chemical evaluation for methylene blue adsorption onto activated carbon, *Afr. J. Manag. Eng. Technol.*, 2(1), 51–62
- Husaini, M. and Ibrahim, M. B. (2025) Adsorption of cationic and anionic dyes in single and binary adsorption of cationic and anionic dyes onto activated carbon derived from agricultural waste. *J. Mater. Environ. Sci.*, 16(5), 881–893.
- Isah A. G., Auta M., Hassan A. (2024) Thermodynamic modeling of methylene blue adsorption onto activated carbon from biomass precursors, *J. Mater. Environ. Sci.*, 15(6), 699–708.
- Jaafar A., El Ayouchia H.B., Lakbaibi Z., A Boussaoud, S Jodeh, K Azzaoui, *et al.* (2019). Degradation of pollutant dye in aqueous solution using Fenton reaction: a DFT study, *GP Globalize Research Journal of Chemistry*, 3(1), 53–61
- Khalid F., Zhang T., Wang L., Chen X. (2022) Activated carbon from almond shells using an eco-compatible method: Screening, optimization, characterization, and adsorption performance testing, *RSC Adv.*, 12, 10227–10240.
- Latifi S., Saoiabi S., Alanazi M.M., Boukra O., Krime A., El Hammari L., *et al.* (2025) Low-Cost Titania-Hydroxyapatite (TiHAp) nanocomposites were synthesized for removal of Methylene blue under Solar and UV irradiation, *Next Materials*, 8, 100859

- Luoyang Y., Wang H., Yong W., Li J., Li X., Zhang G. (2024) Blue coke-based activated carbon adsorbents: Insights into the efficiency and mechanism of methylene blue removal, *Arab. J. Chem.*, 17, 105898.
- McCaffrey Z., Torres L. F., Chiou B.-S., Hart-Cooper W., McMahan C., Orts W. J. (2024) Almond and walnut shell activated carbon for methylene blue adsorption, *ACS Sustain. Resour. Manag.*, 1(7), 1421–1431.
- N'diaye A.D., Hammouti B., Nandiyanto A.B.D., Al Husaeni D.F. (2022), A review of biomaterial as an adsorbent: From the bibliometric literature review, the definition of dyes and adsorbent, the adsorption phenomena and isotherm models, factors affecting the adsorption process, to the use of Typha species waste as a low-cost adsorbent, *Communications in Science and Technology*, 7 No.1, 140-153
- Oliveira L. C. A., Pereira M. C., Silva M. A. P., Soares J. E. (2020) Characterization of activated carbon derived from biomass and its application in dye adsorption, *J. Environ. Chem. Eng.*, 8(1), 103572.
- Rabiu, M. A., Husaini, M., Usman, B., Ibrahim, M. B. (2023) Adsorption of Basic Magenta Dye From Aqueous Solution Using Raw And Acid Modified Yam Peel As Adsorbent. *Bayero Journal of Pure and Applied Sciences*. 14(1), 460 – 466.
- Rashidi N. A., Yusup S. (2022) FTIR and SEM analyses of activated carbon produced from agricultural waste: Structural changes before and after adsorption, *Environ. Nanotechnol. Monit. Manag.*, 17, 100630.
- Ren, G., Li, Z., Fu, P. (2024) Preparation and application of walnut shell-based activated carbon for methylene blue removal: Kinetic and thermodynamic studies. *Biomass Conversion and Biorefinery. Advance online publication*. 14(6), 8937-8954.
- Rial A., Jiménez V., Ortega A. (2024) Adsorptive removal of methylene blue using almond shell-derived activated carbon: Equilibrium and thermodynamic evaluation, *Chem. Eng. J.*, 474, 145042.
- Saeed M., Muneer M., Haq A. U., Akram N. (2022) Photocatalysis: an effective tool for photodegradation of dyes—a review, *Environ. Sci. Pollut. Res.*, 29, 293–311.
- Shahcheragh S. K., Mohagheghi M. M. B., Shirpay A. (2023) Effect of physical and chemical activation methods on the structure, optical absorbance, band gap and Urbach energy of porous activated carbon, *SN Appl. Sci.*, 5, Article 313.
- Smith J. D., Lee A. T. (2024) Proximate analysis of biomass feedstocks: Standards, applications, and implications for activated carbon quality, *Biomass Bioenergy*, 185, 108212.
- Yagub M. T., Sen T. K., Afroze S., Ang H. M. (2021) Mechanistic understanding of methylene blue adsorption onto biomass-derived activated carbons: Role of functional groups and surface interactions, *Chemosphere*, 272, 129688.
- Zhao X., Li J., Wang Y. (2022) Review on methylene blue: Its properties, uses, toxicity and removal methods, *Water*, 14(2), 242.
- Zhou L., Chen W., Zhang Z., Li Y. (2023) Functional group evolution in carbonaceous adsorbents revealed by FTIR: A study of dye uptake mechanisms, *J. Mol. Liq.*, 381, 121740.

(2025); <http://www.jmaterenvironsci.com>